



TITLE:

# 気象レーダーと分布型流出モデルを用いた洪水予測システム

AUTHOR(S):

キム, スンミン; 立川, 康人; 寶, 馨

---

CITATION:

キム, スンミン ...[et al]. 気象レーダーと分布型流出モデルを用いた洪水予測システム. 京都大学防災研究所年報. B 2006, 49(B): 55-65

ISSUE DATE:

2006-04-01

URL:

<http://hdl.handle.net/2433/26595>

RIGHT:

## Flood Forecasting System Using Weather Radar and a Distributed Hydrologic Model

Sunmin KIM \*, Yasuto TACHIKAWA, Kaoru TAKARA

\* Graduate School of Urban and Environmental Engineering, Kyoto University

### Synopsis

A real-time flood forecast system is proposed with stochastic radar rainfall forecasts and recursive measurement update in a distributed hydrologic model. In the first part of the system, a radar image extrapolation model gives deterministic rainfall predictions and error fields are simulated to offer probable variation on the deterministic predictions. The error field simulation uses a random field generation method based on an analyzed error structure of the current time rainfall prediction. Then, the probable rainfall fields with generated error fields are given to a distributed hydrologic model to achieve an ensemble runoff prediction. In the second part of the system, the distributed model is coupled with the Kalman filter to utilize online hydrologic information by several techniques including Monte Carlo simulation scheme.

**Keywords:** flood forecasting, weather radar, distributed hydrologic model

### 1. Introduction

The nature is composed of infinite process, and each process is surely deterministic (out of mention for the micro process on the level of quantum physics, which is under the uncertainty principle of Heisenberg, 1927), but affected by uncountable number of factors. What we are trying to do with modeling is to find the most dominating factors on a process and to simplify the process with an understandable structure which is composed of those several effective and observable factors.

For any natural phenomenon that we are trying to forecast, if the spatiotemporal boundary or initial condition were exactly known, and if the model exactly simulated the process, then the computed phase path would provide an exact forecast. But, unfortunately, neither assumption is valid based on current technology or knowledge. One should bear in mind that there are always initial error in a model at the beginning of simulation and there are always additional error during a

simulation generated by the imperfect model structure. To estimate the effect of those errors on the forecast results, it is necessary to supplement such deterministic forecasts with detailed information by estimates of forecast reliability. By this reason, the stochastic concept has been included in forecasting, and ensemble simulation has been used as a good tool for carrying those stochastic concepts in a computer simulation.

Recent trends of flood forecast are away from the conventional deterministic forecasts of hydrographs toward offering probabilistic forecasts, which include its prediction uncertainty. Deterministic flood forecast specifies a point estimate of the predicted values, such as precipitation and river stages/discharges. On the other hand, a stochastic forecast specifies a certain probability distribution function of the predicted values. The predictive probability in a probabilistic forecast is a numerical measure of the certitude degree about the intensity of a flood event, based on all meteorological or hydrological information utilized in the forecasting process (R. Krzysztofowicz, 2001).

This study discuss about a stochastic forecasting based on an ensemble simulation and presents a real-time flood forecast algorithm, which is built in a probabilistic way, with weather radar and a distributed hydrologic model. The algorithm mainly consists of two parts; probable rainfall forecast with a radar image extrapolation model and state variables update in a distributed hydrologic model.

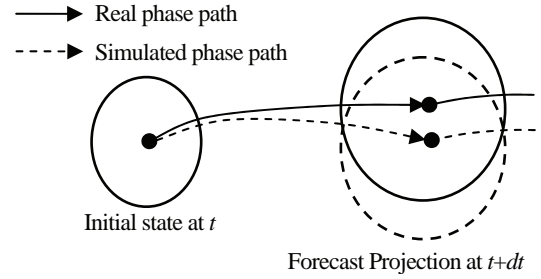
## 2. Stochastic Forecasting by Ensemble Simulation Method

### 2.1 Historic Ensemble Simulation

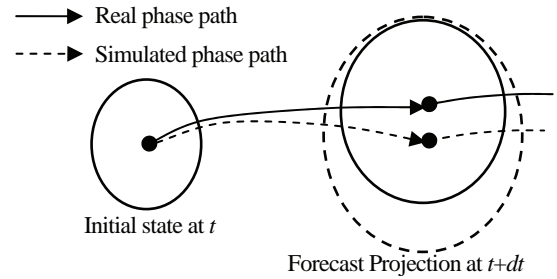
In atmospheric modeling, stochastic dynamic forecast was introduced more than three decades ago (Epstein, 1969). Until now, main purpose of ensemble forecasting in those models is to consider uncertainties of initial conditions and boundary conditions at the beginning of forecasting. After Lorenz (1963) found that only slightly different initial conditions yield quite different results in a numerical weather prediction model, small perturbation of initial condition in a beginning of model simulation has been used as a trigger of an ensemble forecasting. One good example of short-range ensemble forecasting of precipitation with well-documented review can be found in Due and Mullen (1997).

Most of ensemble simulations in early stage are concerned only the internal growth of error arising from the difference in initial conditions and ignore the external growth of error arising from the difference between a numerical model and the real atmosphere (Leith, 1974). Until now, ensemble simulation for a probabilistic forecasting is criticized of its underestimation of the total uncertainty because not all sources of uncertainty are accounted for in the ensemble generator (Krysztowicz, 2001). Because of the improper model structure, which is carrying the simulation, there is always a chance that the initiated variant initial conditions for an ensemble simulation have resulted in different forecast projection (Fig. 1).

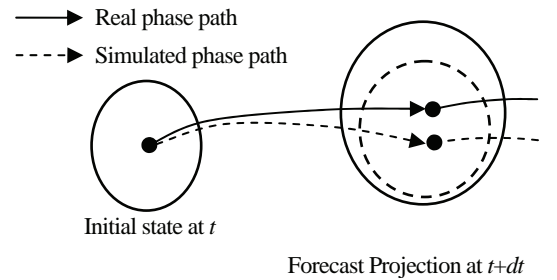
Figure 1 presents schematic drawings of ensemble forecasting, plotted in terms of an idealized two-dimensional phase space. The first circles at initial time  $t$  represent initial states for ensemble forecasting, and a dot stands for the best guess or the best observation at the beginning of the simulation. The solid line represents phase path of the states by the process in the



(a) Forecasted result from a model gives shifted projection to the real projection at  $t+dt$ .



(b) Model gives diverged projection.



(c) Model gives localized projection.

**Fig. 1** Three different cases of forecast projection caused by variant simulation situations or variant models

real nature, and the dashed line stands for the phase path of model simulations. Because of the imperfectness of a model, the forecast projection, which is represented by dashed line circle, can have shifted space to the real projection (solid line circle) as shown in Figure 1 (a). In other cases, the forecast projection can have diverged state space (Figure 1 (b)) or it can converged in a limited space area (Figure 1 (c)). These three cases can be happen in different model running or in different situations in one-model simulation. In any case, as forecasting goes on for  $t+ndt$ , the shifting or divergence of the simulation would make much bigger discrepancy to the real phenomena.

## 2.2 Proposed Ensemble Simulation Method

If any model shows one specific pattern of discrepancy and if it can be recognizable, the model structure should be corrected for improving the forecasting behavior. If any model shows variant discrepancy pattern on a different simulation time or condition, which is more common in model simulations, the different forecast projection should be corrected by updating the model state vectors with the most recent observations. This kind of real-time updating can be fulfilled by adopting a data assimilation method, such as Kalman filter, or additional error simulation model.

As a step towards addressing the updating of state vectors during an ensemble simulation, this study proposes a real-time forecasting algorithm using weather radar and a distributed hydrologic model. The algorithm mainly consists of two parts; probable rainfall forecast with a radar image extrapolation model and state variables update in a distributed hydrologic model. Brief illustrations for the proposed algorithm are as below.

First, a new attempt of ensemble rainfall forecast is carried out with radar rainfall prediction and spatial random error field simulation (Kim *et al.*, 2006). The radar extrapolation model gives a deterministic rainfall prediction, then its prediction error structure is analyzed by comparing with the observed rainfall fields. With the analyzed error characteristics, spatial random error fields are simulated using covariance matrix decomposition method. The simulated random error fields, which successfully keep the analyzed error structure, improve the accuracy of the deterministic rainfall prediction. Then, the random error fields with the deterministic fields are given to a distributed hydrologic model to achieve an ensemble runoff prediction.

Second, a Kalman filter (Kalman, 1960) is coupled with a distributed hydrologic model to update spatially distributed state variables and to incorporate the uncertainty of rainfall forecast data (Kim *et al.*, 2005). Here, rather than attempting an impractical algorithm formulation, several techniques are newly adopted. In the measurement update algorithm, the discharge and storage amount relationship is used as the observation equation, and the ratio of total storage amount was applied for setting the water stage for each cell in the distributed hydrologic model. For the prediction algorithm, a Monte Carlo simulation is adopted to propagate the state variable and its error covariance.

## 3. Short-term Rainfall Forecast Using Weather Radar

### 3.1 Translation Model

Translation model (Shiiba *et al.*, 1984), which is one of radar image extrapolation models, simulates short-term rainfall forecasts in this study. In this model, the horizontal rainfall intensity distribution,  $z(x,y,t)$  with spatial coordinate  $(x,y)$  at time  $t$  is represented as:

$$\frac{\partial z}{\partial t} + u \frac{\partial z}{\partial x} + v \frac{\partial z}{\partial y} = w \quad (1)$$

$$\text{here } u = \frac{dx}{dt}, \quad v = \frac{dy}{dt}, \quad w = \frac{dz}{dt}$$

where,  $u$  and  $v$  are advection velocity along  $x$  and  $y$ , respectively, and  $w$  is rainfall growth-decay rate along time. Characteristic of the translation model is that the vector  $u$ ,  $v$ , and  $w$  are specified on each grid in a manner of:

$$\begin{aligned} u(x, y) &= c_1 x + c_2 y + c_3 \\ v(x, y) &= c_4 x + c_5 y + c_6 \\ w(x, y) &= c_7 x + c_8 y + c_9 \end{aligned} \quad (2)$$

so that the advection velocities can express the patterns of non-uniform movement of rainfall, such as rotation and sheer strain (Takasao *et al.*, 1994). The parameters  $c_1 \sim c_9$  are sequentially optimized using observed rainfall data by the square root information filter.

The translation model provides expected rainfall movements under the assumption that the vectors  $u$  and  $v$  are time invariant for the next several hours and that there is no growth-decay of rainfall intensities during that time. In this research, three consecutive observed rainfall fields, which have 3km and 5min of resolution, are used to determine  $u$  and  $v$ . When forecasting rainfall fields, the  $u$  and  $v$  are assumed spatially uniform. In a real nature, the rainfall movement would have spatially invariant movements. However, most of rainfall in Japan, which happens during rainy season and Typhoon season, has frontal rain band over wide area so that the movement of the rainfall band can be treated as a uniform movement in a single radar range.

### 3.2 Prediction Error Structure Analysis

Tachikawa *et al.* (2003) statistically analyzed the characteristics of absolute prediction error and relative prediction error defined as Equations 3 and 4.

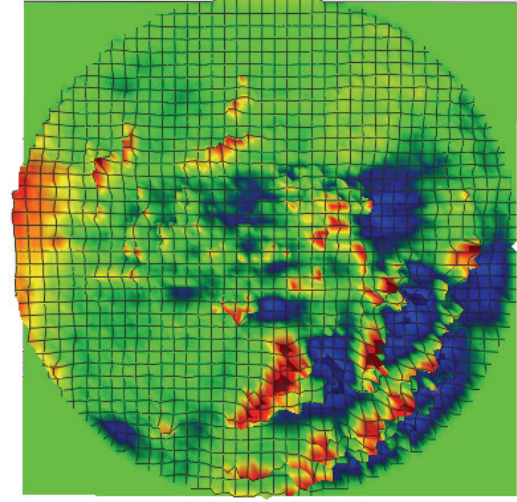
$$E_{a,i} = R_{o,i} - R_{p,i} \quad (3)$$

$$E_{r,i} = (R_{o,i} - R_{p,i}) / R_{p,i} \quad (4)$$

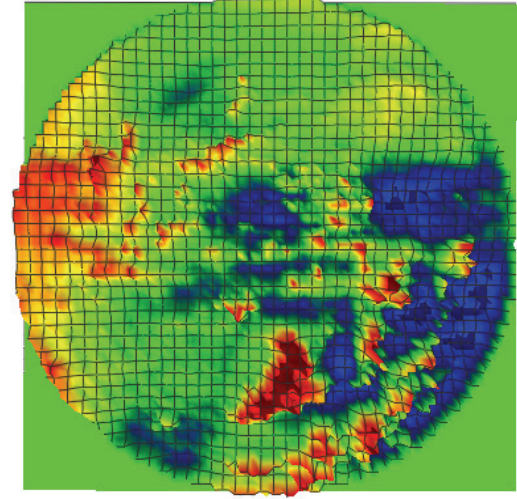
The absolute prediction error  $E_{a,i}$  on a certain grid  $i$  is calculated from the difference between predicted rainfall  $R_{p,i}$  and observed rainfall  $R_{o,i}$  on the grid, while the relative prediction error  $E_{r,i}$  is the ratio of the absolute prediction error to its predicted rainfall. Tachikawa *et al.* (2003) examined the timely accumulated error values with variant spatial resolutions and found that the distributions of absolute and relative error are respectively close to normal distribution and lognormal distribution. This study concentrate on the absolute prediction error  $E_{a,i}$  and simulate the spatial random error fields of possible  $E_{a,i}$  on the future prediction target time on a real-time basis.

Spatial correlation coefficients of absolute prediction error, which shows how much the error is spatially correlated to each other, is calculated by grouping every pair of the absolute error values on each error field. The correlation coefficients shows high values for close distance and decrease, as the distance gets longer. It is found that the absolute error from longer prediction time has higher values, and the values are almost diminished around 15km in most prediction cases. More details of error structure analysis can be found in Kim *et al* (2005).

Similar to the other extrapolation models, the translation model usually ignores the growth and decay of the rainfall intensities or nonlinear motion of rainfall bands. To forecast precipitation accurately, however, it needs to understand not only the exact rain band movement but also the generation, growth, and decay of rain cell, particularly in mountainous regions such as in Japan. For checking of the relationship between topographic pattern and rainfall prediction error, which is mainly caused by the ignorance of the growth and decay of rain cell, absolute prediction error was calculated and accumulated on every grid. The absolute prediction error  $E_{a,i}$  on grid  $i$  was calculated from the difference between predicted rainfalls  $R_{p,i}$  and observed rainfalls  $R_{o,i}$  on the grid ( $E_{a,i} = R_{o,i} - R_{p,i}$ ). As shown in Figure 2, there were



(a) Accumulated 60min prediction error



(b) Accumulated 120min prediction error

**Fig. 2** Accumulated prediction error (Observed at Miyama radar station, Japan on June 1993)

certain spatial patterns of prediction error on each accumulation. It was also found that different wind direction gives different spatial pattern of the prediction error through the same test on other rainfall events. The frequency distribution of the absolute error follows a normal distribution.

### 3.3 Simulation of Prediction Error

The main part of the error field simulation algorithm is to simulate possible error fields of the future prediction using the current prediction error structure, assuming temporal persistency of the error characteristics from the current time to the prediction target time. The proposed scheme is using certain



duration of prediction error data for the simulation of future prediction error as shown in Figure 3.

In the figure, the observed rainfall fields, the previous prediction fields, and the prediction error fields are sequentially illustrated until the current time  $t$ . There would be various prediction fields on each time by various prediction lead-times. However, for the simplicity, only one prediction with the lead-time  $\Delta t$  is considered in the figure. Again, every prediction field at each time step is the prediction results that are carried at  $\Delta t$  time before of that time step. At the current time  $t$ , the translation model carries another prediction for the time  $t+\Delta t$  and the probable prediction error of the prediction at  $t+\Delta t$  is trying to be simulated with the current error characteristics.

The current characteristics of the prediction error can be presented by basic probabilistic statistics under an assumption that time series of the error on each grid follows normal probability distribution. Here, the basic statistics stand for mean and standard deviation values of the most recent error in certain duration, last one hour for example, on each grid. Based on this simple procedure, the statistic fields can compromise spatial and temporal pattern of the current errors and these can be updated on real-time basis. If the spatiotemporal characteristic of the prediction error lasts for couple of hours, therefore the statistic characteristics of the error on the prediction target time  $t+\Delta t$  are similar to the characteristics of the current statistic fields, the possible error fields at  $t+\Delta t$  can be simulated by using the current statistic fields.

The statistic field, the mean and standard deviation field of error, make it possible to compromise the spatial and temporal pattern of the most recent prediction errors, and it can be updated on a real-time basis. The statistic field was then converted to spatially correlated random values to the probable error field by Equation 5, which is the goal of the error filed simulation.

$$\begin{bmatrix} E_{s,1} \\ E_{s,2} \\ E_{s,3} \\ \vdots \\ E_{s,n} \end{bmatrix} = \begin{bmatrix} sd_1 & 0 & 0 & \cdots & 0 \\ 0 & sd_2 & 0 & \cdots & 0 \\ 0 & 0 & sd_3 & \cdots & 0 \\ \vdots & \vdots & \vdots & \ddots & \vdots \\ 0 & 0 & 0 & \cdots & sd_n \end{bmatrix} \begin{bmatrix} y_1 \\ y_2 \\ y_3 \\ \vdots \\ y_n \end{bmatrix} + \begin{bmatrix} m_1 \\ m_2 \\ m_3 \\ \vdots \\ m_n \end{bmatrix} \quad (5)$$

Here, the  $m_i$  and  $sd_i$  are the mean and standard deviation of the current prediction error on the grid  $i$ , respectively. The  $y_i$  is the unit random error of the vector  $\mathbf{Y}$ , which is a

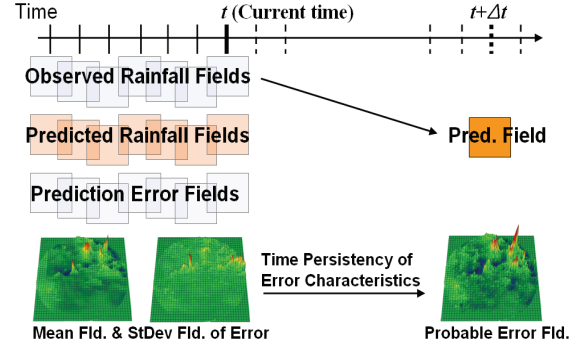


**Fig. 3** Schematic illustration of the probabilistic error field simulation using statistic error fields and error persistency assumption

set of spatially correlated random values with zero mean and unit standard deviation;  $N(0,1)$ . The vector  $\mathbf{Y}$  was generated using spatial correlation of the current error by the covariance matrix decomposition method of Davis (1980). The  $E_{s,i}$  is the simulated error for the prediction target time. Equation 5 is a linear equation, thus the spatial correlation structure of  $\mathbf{Y}$ , which was obtained from the  $E_a$ , was maintained in the  $E_s$ . Generation of many sets of  $\mathbf{Y}$  made it possible to get many target error fields.

### 3.4 Generation of Extended Prediction Fields

Deterministic prediction from the translation model is extended to many possible prediction rainfall fields by combination with the simulated error fields in a form of:

$$R_{e,i} = R_{p,i} + E_{s,i} \quad (6)$$

where,  $E_{s,i}$  is the simulated prediction error value on grid  $i$ ,  $R_{p,i}$  is the deterministic prediction from the translation model, and  $R_{e,i}$  is the extended prediction. Because the simulated error keeps the error statistics of the absolute prediction error ( $E_{s,i} \approx E_{a,i}$ ), the extended prediction can be close to the observed rainfall on the prediction target time. In other words, the properly simulated prediction error can improve the accuracy of the deterministic prediction.

Negative values could occur on the extended prediction field, since some values on the simulated error field could have a negative value, which can be larger

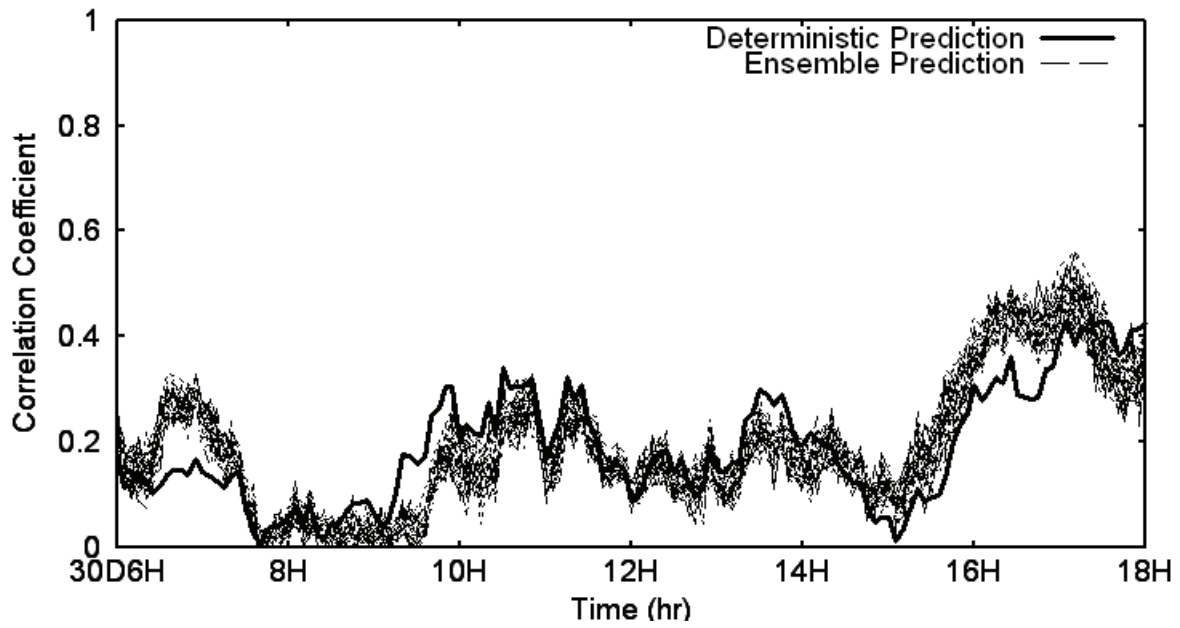


**Fig. 4** Correlation coefficient to observation of deterministic and extended prediction  
(Results are from the testing with the Miyama radar station data).

than the deterministic prediction rainfall value on that point. This negative rainfall set to zero, and the same amount of negative values compensated the positive rainfall values for keeping the total rainfall amount.

Evaluation with correlation coefficient of observation and extended prediction using the extended 60min prediction fields are presented in Figure 4. The coefficient values from the extended prediction show more improved results than from the deterministic prediction.

#### **4. Distributed Hydrologic Model, CDRMV3 with Kalman Filter**

The objective of the real-time update algorithm was to couple the Kalman filter (Kalman, 1960) to a physically based distributed model for recursive state variables updating and for incorporating of rainfall input data uncertainty into the simulated discharge output data. The model used here is the Cell-based Distributed Runoff Model Version 3 (CDRMV3, Kojima *et al.*, 2003). The model solves the one-dimensional kinematic wave equations for both subsurface flow and surface flow using the Lax-Wendroff scheme on every computational node in a cell. Discharge and water depth propagate to the steepest downward adjacent cell according to a flow direction map generated from DEM data. The flow direction map that defines the routine order for water

flow propagation in CDRMV3 is prepared by the conventional eight-direction method. A specified stage-discharge relationship, which incorporates saturated and unsaturated flow mechanism, was included in each cell (Tachikawa *et al.*, 2004). The stage-discharge relationship is expressed by three equations corresponding to the water levels divided into three layers.

##### **4.1 Updating Spatially Distributed Water Depth**

To minimize the discrepancy between simulation output and observed discharge, correcting the model internal state variables is the commonly used updating scheme in real-time simulation. However, in updating the measurement for a distributed hydrologic model, not only the magnitude of the state variable but also its spatial distribution pattern should be considered. During a rainfall-runoff simulation, inappropriate rearrangement of spatial distribution of state variables produces obvious effects on the runoff simulation results (Kim *et al.*, 2004).

To avoid an unpredictable collapse of the internal model state during a simulation, the update method we used retains the spatial distribution pattern of the state variables before and after the updating as shown in Figure 5. Only the total amount of the state variables was updated by multiplying the variables by a specific factor. This factor was calculated from the ratio of the total storage amount, estimated from

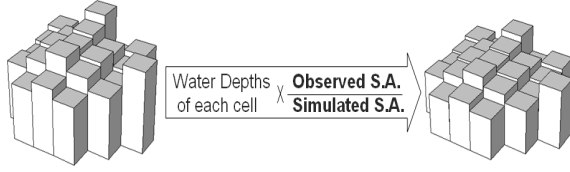


**Fig. 5** Resetting of state variables using the ratio of storage amounts

observed discharge, to the simulated total storage amount. The simulated water depth on every computation node in the model was multiplied by the calculated factor, and the model retained the spatial distribution pattern of the internal state variables.

To calculate the ratio of total storage amount, both the simulated and observed storage amounts must be acceptably accurate. Simulated total storage amount in a model is easily calculated from each water depth on each grid cell by multiplying by its cell area. However, because the total storage amount cannot be measured directly, the corresponding total storage amount must be estimated from the observed discharge, assuming a discharge–storage relationship. To relate discharge at the basin outlet  $Q$  and the total storage amount  $S$ , the  $Q$ – $S$  relationship under a steady-state assumption was used. Applying a constant rainfall intensity over the study basin until it reached a steady state, one pair of total storage amount and discharge values was acquired from the CDRMV3. Applying variable rainfall intensities, the  $Q$ – $S$  relationship can be obtained. A runoff simulation under unsteady-state conditions produced a loop-shaped  $Q$ – $S$  relationship, and the curve differed from event to event, but the difference of the total storage amount obtained from the curves of the steady state and unsteady-state condition was not significant. Moreover, instead of direct conversion of observed discharge to the storage amount, the storage amount  $S_{o,t}$  at time step  $t$  was obtained as

$$S_{o,t} = S_{s,t} + H(Q_{o,t} - Q_{s,t}) \quad (7)$$

where,  $S_{s,t}$  and  $Q_{s,t}$  are, respectively, total storage amount and the outlet discharge simulated by the model at time step  $t$ ,  $Q_{o,t}$  is the observed discharge at the outlet, and  $H$  is the mean of the gradient values on the  $Q$ – $S$  relationship at the point defined by  $S_{s,t}$  and

$Q_{s,t}$ . The calculated total storage amount  $S_{o,t}$  from Equation 7 was regarded as the observed total storage amount.

Since the calculated ratio from the storage amounts represented the ratio of average water depth in a catchment, this ratio was applied to the simulated water depth on every grid cell to rearrange the distributed storage amount. After this procedure, the updated water depths were equivalent to the storage amount  $S_{o,t}$  estimated from the observed discharge. The spatial distributed pattern of water depth contained the predicted water storage pattern before updating, and the pattern reflected the spatial distribution of rainfall and topographic properties.

#### 4.2 Kalman Filter Coupling with CDRMV3

In the measurement update algorithm of the Kalman filter, an observation vector  $y_k$  at time step  $k$  is described as a linear vector function of a state vector  $x_k$ , and observation noise vector  $w_k$  assuming white noise is included in the observation as:

$$y_k = H_k x_k + w_k, \quad w_k \sim N(0, R_k) \quad (8)$$

which has an error covariance matrix  $R_k$ . The  $m \times n$  matrix  $H$  relates the state vector to the observation. The state variables are updated as follows:

$$\begin{aligned} \hat{x}(k|k) &= \hat{x}(k|k-1) + K_k (y_k - H_k \hat{x}(k|k-1)) \\ P(k|k) &= P(k|k-1) - K_k H_k P(k|k-1) \\ K_k &= P(k|k-1) H_k^T (H_k P(k|k-1) H_k^T + R_k)^{-1} \end{aligned} \quad (9)$$

The difference,  $y_k - H_k \hat{x}(k|k-1)$ , which is called the residual or innovation, reflects the discrepancy between the estimated observation  $H_k \hat{x}(k|k-1)$  and the actual observation  $y_k$ . In the measurement update algorithm, the state vector  $\hat{x}(k|k-1)$  and its error covariance vector  $P(k|k-1)$  as estimated at time step  $k-1$ , are updated by use of the  $m \times n$  matrix  $K_k$  at time step  $k$ . The matrix  $K_k$ , called Kalman gain, is chosen to minimize the updated error covariance  $P(k|k)$ . In the algorithm, the superscript ‘ $\wedge$ ’ indicates estimated value and ‘ $T$ ’ indicates the transpose of a matrix.

Here, the observation equation is the  $Q$ – $S$



relationship, thus the scalar value of  $H$  represents the gradient of the  $Q$ - $S$  relationship using the simulated results at the updating time step. The results from the measurement update algorithm were used to update the total storage amount of the study basin and its error variance. With the updated watershed storage amount, the ratio method described in the previous section was used to update the spatial distribution of water depth in the distributed hydrologic model.

In the Kalman filter,  $n \times n$  matrix  $F$  in the system equation:

$$x_{k+1} = F_k x_k + B_k + v_k; \quad v_k \sim N(0, Q_k) \quad (10)$$

relates the state variables  $x$  at the current time step  $k$  to those at the next step  $k+1$ . The system is continuously affected by white Gaussian system noise,  $v_k$ , with system error covariance matrix  $Q_k$ . The matrix  $B_k$  provides optional control input to the state  $x$ . The time update algorithm

$$\begin{aligned} \hat{x}(k+1|k) &= F_k \hat{x}(k|k) + B_k \\ P(k+1|k) &= F_k P(k|k) F_k^T + Q_k \end{aligned} \quad (11)$$

is used to project forward the current state and the  $n \times n$  error covariance to obtain estimates for the next time step.

In the CDRMV3, a complicated relationship exists between the present and the next time-step state variable, *i.e.*, the present and the next time-step total storage amount. The current water depth at each cell responds interdependently to the next step's water depth according to the current spatial distribution of water depth and rainfall input. It is impractical to define the system matrix  $F_k$  to formally express this process from the hydrologic system equations. However, use of the Monte Carlo simulation method (see Figure 6) made it possible to project the nonlinear variation of system states and their error covariance without the need for linearized system equations. Evensen (1994) showed that Monte Carlo methods permit the derivation of forecast error statistics in the Kalman filter algorithm and thus, the inefficiency involved in the linearization of system states can be eliminated.

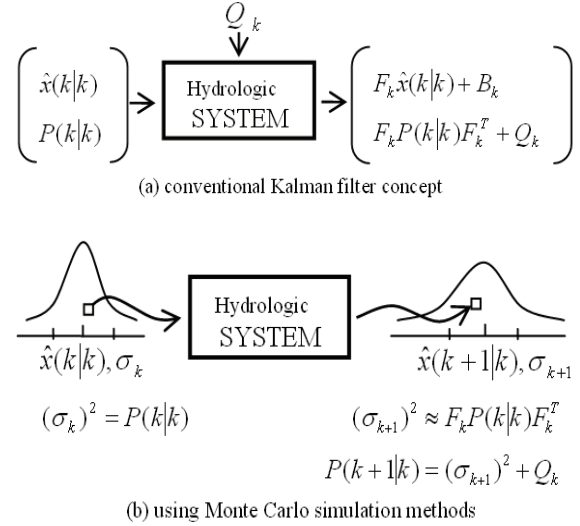


**Fig. 6** Schematic drawing of time update algorithm (a) of the conventional Kalman filter concept and (b) using Monte Carlo simulation methods.

### 4.3 Setting the Uncertainty in Kalman Filter

The most difficult part of applying the Kalman filter to a hydrologic model is determining the covariance of the system and observation noise. Although the Kalman filter provides an algorithm for better forecasting by updating the state estimates, its success depends largely on an appropriate determination of the error statistics, which requires proper judgment by the hydrologist.

The basic assumption of the Kalman filter is that the system and observation noise are both white and Gaussian. This assumption is justified physically when the noise is largely caused by a number of small sources (Mayback, 1979). From this point of view, the observation noise, which is usually corrupted by several definable error sources, can be regarded as a white, Gaussian distribution.

In addition, an accuracy assessment test using data obtained over a long duration makes it possible to properly estimate the measurement error covariance (Kitanidis and Bras, 1980). However, the system error covariance is the critical value for the Kalman filter. It contains many error sources, which are difficult to define separately. The system error covariance should reflect system structure error, parameter identification error, and input data error, as well as system linearization error. Underestimation of

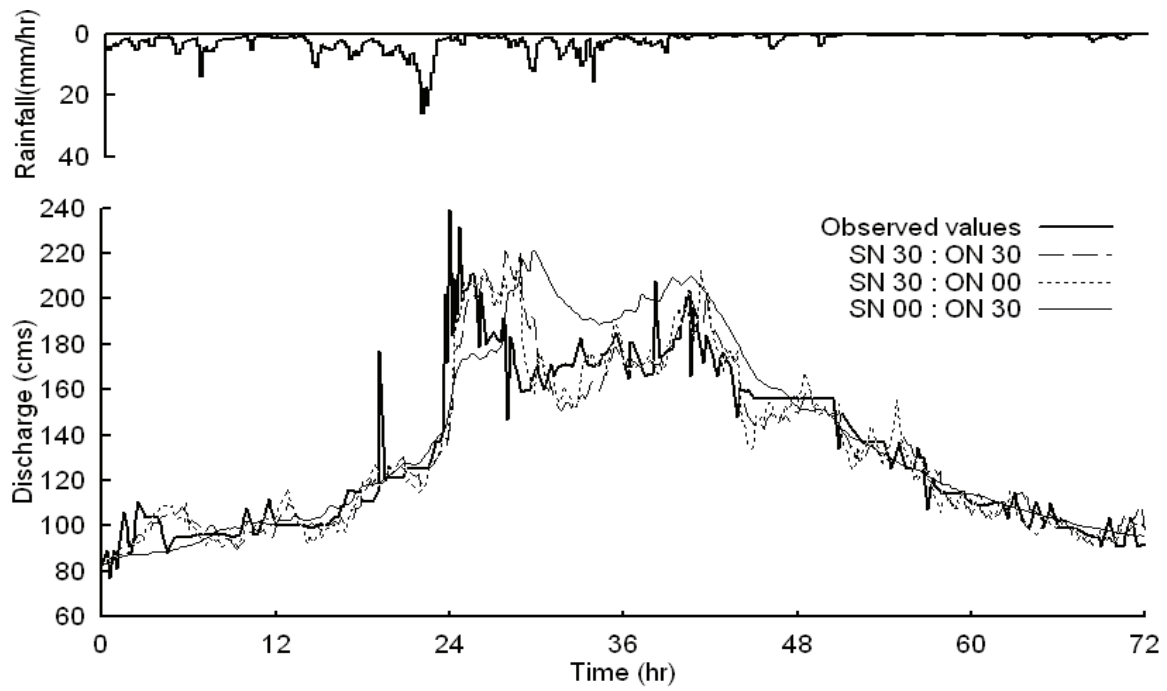


**Fig. 7** Observed and feedback through the Kalman filter under different system and observation noise conditions (The results are from testing at the Kamishiiba Basin, Japan). SN 30 and ON 30 denote the given error covariance in the form of standard deviation of noise in discharge,  $\pm 30 \text{ m}^3/\text{s}$ , and SN 00 and ON 00 mean that no error covariance is given for system and observation, respectively.

the system error leads to excessive confidence in the model behavior, and overestimated system error makes the filter too sensitive to observation values. In practice, the system error covariance is usually estimated by a trial and error procedure assuming it has a constant value.

Because the main purpose of this research was to study a methodology for coupling the Kalman filter to a distributed hydrologic model, several cases of feedback performance with several assumed error covariances were tested. The Kalman filter-coupled with CDRMV3 was tested on the Kamishiiba basin under various error covariance conditions. Figure 7 shows the feedback through the algorithm under the three different error conditions. The filter-coupled CDRMV3 yielded better results than off-line simulations and can, thus, be used as a probabilistic forecast algorithm. Furthermore, the developed algorithm can incorporate the uncertainty of input and output measurement data as well as the uncertainty in the model itself.

## 5. Conclusion Remarks

This study reviewed ensemble forecasting using weather radar and a distributed hydrologic model. Using radar rainfall data in short-term forecasting is a great enhancement for giving fine resolution of input to a distributed hydrologic model. However, even though its powerful usage in operational hydrology, radar image extrapolation model has been hardly used for ensemble simulation so far. On the other hand, historic ensemble forecasting has been criticized for insufficient consideration of total uncertainty. Typical ensemble simulation has been based only on the initial condition uncertainty and usually passing over the structural uncertainty of model.

This study proposes new attempt of ensemble forecasting for the radar extrapolation model with an external error simulation model. The error simulation model continuously analyze the most recent error characteristic and simulate possible error field for the next forecasting. Based on stochastic generation of future error field, the extended rainfall prediction fields offer its reliability range as well as correction of the prediction bias.

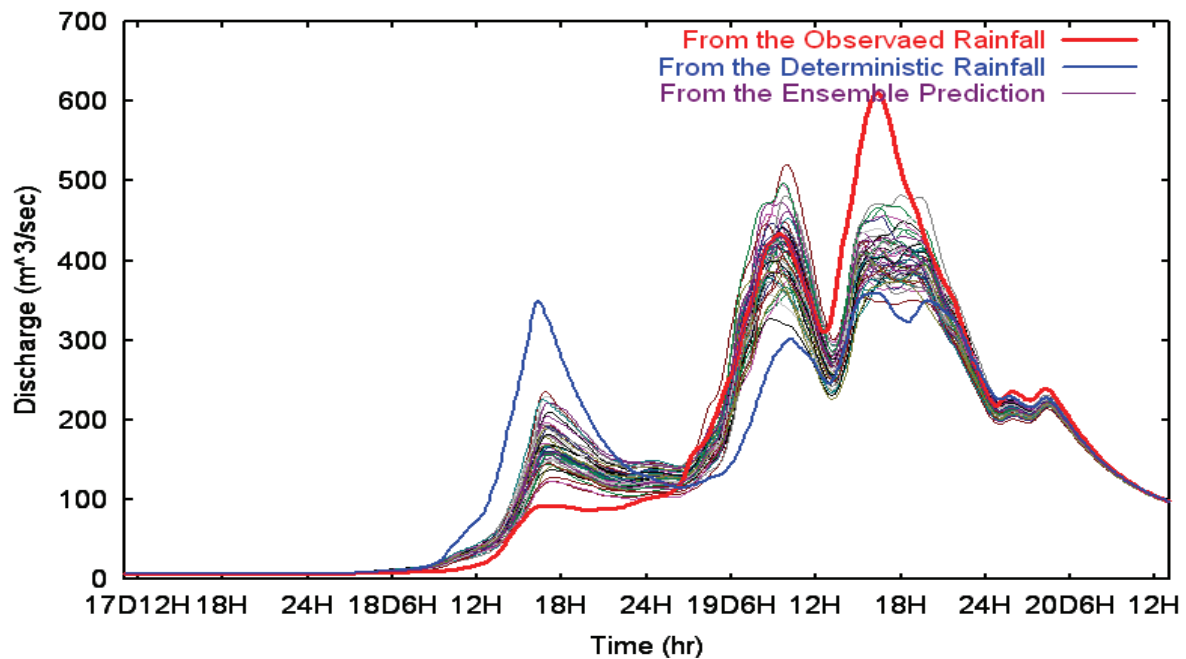


**Fig. 8** Example of an ensemble rainfall-runoff forecasting for 60min ahead (Ieno basin 476km<sup>2</sup>, Japan)  
Rainfall forecasting is done by radar observed data during 17- 20, August 1992.

Figure 8 shows one good example of improved ensemble rainfall-runoff simulation using the proposed method. The red line stands for the discharge generated from the observed radar data. The blue line is the discharge hydrograph from the deterministically forecasted rainfall using the translation model. The purple lines are from the extended rainfall forecasting, which is generated using the error simulation model. The forecasting is for 60min forehead. It can be clearly seen that the discharge results from the ensemble forecasting give much improved runoff simulation results.

Moreover, distributed model can give us its improved runoff simulation performances when it is coupled with recursive state variables update algorithm, such as Kalman filter proposed in this study. Stochastic real-time flood forecasting system, using radar extrapolation with error simulation model and the Kalman filter coupled distributed hydrologic model, can give us improved forecasting accuracy and reliable ensemble ranges. The developed real-time forecasting algorithm is under working for applying on the Gam-cheon Basin, South Korea with Typhoon Rusa flood events in 2002, which was one of the most disastrous flood disasters in South Korea.

## References

- Davis, M. W. (1987): Generating large stochastic simulation-The matrix polynomial approximation method, *Mathematical Geology*, Vol. 19, No. 2, pp. 99-107.
- Du, J. and Mullen, S. L. (1997): Shot-range ensemble forecasting of quantitative precipitation, *Monthly Weather Rev.*, Vol.125, pp. 2427-2459.
- Epstein, E. S. (1969): Stochastic dynamic prediction, *Tellus*, Vol 21, pp. 739-759.
- Evensen, G. (1994): Sequential data assimilation with a nonlinear quasi-geostrophic model using Monte Carlo methods to forecast error statistics, *Journal of Geophysical Research*, Vol. 99, pp. 10143-10162.
- Heisenberg, W. (1927): Über den anschaulichen Inhalt der quantentheoretischen Kinematik und Mechanik, *Zeitschrift für Physik*, Vol 43, pp. 172-198, English translation: Wheeler, J. A. and Zurek, H. (1983): *Quantum Theory and Measurement*, Princeton Univ. Press, pp. 62-84.
- Kalman, R. E. (1960): A new approach to linear filtering and prediction problems, *Transaction of the ASME – Journal of Basic Engineering*, Vol. 83, pp. 35-45.
- Kim, S., Tachikawa, Y., and Takara, K. (2004): Real-time updating of state variables in a distributed hydrologic model, *Annals of Disaster Prevention Research Institute, Kyoto Univ.*, Vol. 47B, pp. 273-282.
- Kim, S., Tachikawa, Y., and Takara, K. (2005): Real-time prediction algorithm with a distributed hydrological

- model using Kalman filter, Annual journal of hydraulic engineering, JSCE, No. 49, pp. 163-168.
- Kim, S., Tachikawa, Y., and Takara, K. (2006): Ensemble rainfall-runoff prediction with radar image extrapolation and its error structure, Annual journal of hydraulic engineering, JSCE, No. 50, CD-ROM.
- Kitanidis, P. K. and Bras R. L. (1980): Real-time forecasting with a conceptual hydrologic model – 1. Analysis of uncertainty, Water Resources Research, Vol. 16, No. 6, pp. 1025-1033.
- Kojima, T. and Takara, K. (2003): A grid-cell based distributed flood runoff model and its performance, Weather radar information and distributed hydrological modeling (Proceedings of HS03 held during IUG2003 at Sapporo, July 2003), IAHS Publ. No. 282, pp. 234-240.
- Krzysztofowicz, R. (2001): The case for probabilistic forecasting in hydrology, Journal of Hydrology, Vol. 249, pp. 2-9.
- Leith, C. E. (1974): Theoretical skill of Monte Carlo forecasts, Monthly Weather Rev., Vol.102, pp. 409-418.
- Lorenz, E. N. (1969): Atmospheric predictability as revealed by naturally occurring analogues. J. Atmos. Sci., Vol. 26, pp. 636-646.
- Maybeck, Peter S. (1979): Stochastic Models, Estimation, and Control, Volume 1, Academic Press, New York.
- Shiiba, M., Takasao, T. and Nakakita, E. (1984): Investigation of short-term rainfall prediction method by a translation model, Jpn. Conf. on Hydraul., 28th, pp. 423-428.
- Tachikawa, Y., Komatsu, Y., Takara, K. and Shiiba, M. (2003): Stochastic modeling of the error structure of real-time predicted rainfall and rainfall field generation, Weather Radar Information and Distributed Hydrological Modelling (ed. by Y. Tachikawa, B. E. Vieux, K. P. Georgakakos & E. Nakakita), IAHS Publ., No. 282, pp. 66-74.
- Tachikawa, Y., Nagatani, G., and Takara, K. (2004): Development of stage-discharge relationship equation incorporating saturated-unsaturated flow mechanism, Annual Journal of Hydraulic Engineering, JSCE, Vol. 48, pp. 7-12.
- Takasao, T., Shiiba, M. and Nakakita, H. (1994): A real-time estimation of the accuracy of short-term rainfall prediction using radar, Stochastic and Statistical Methods in Hydrol. and Environm. Eng., Vol.2, pp. 339-351.

## 気象レーダーと分布型流出モデルを用いた洪水予測システム

キム, スンミン\*・立川康人・寶 馨

\*京都大学大学院工学研究科都市環境工学専攻

### 要旨

気象レーダーを用いた確率的な降雨予測手法と観測更新手法を導入した分布型流出モデルとを組み合わせた実時間洪水予測システムを開発する。まず始めにレーダー降雨データを外挿して得られる決定論的な降雨予測値に降雨場の予測誤差を導入し、起こり得る多数の予測降雨場を発生させる。予測誤差は、現在時刻の予測誤差特性を反映させた確率場モデルによって発生させる。次に、発生させた多数の降雨場を分布型流出予測モデルに入力し、河川流量のアンサンブル予測を実施する。分布型流出予測モデルにはカルマンフィルターを導入し、オンラインで入手できる水文情報をモデル状態量に反映させる。分布型流出予測モデルにカルマンフィルターを適用するに当たっては、状態量の観測更新・予測更新のためにモンテカルロシミュレーションを始めとしていくつかの工夫を施している。

**キーワード:**洪水予測, 気象レーダー, 分布型流出モデル